This is the accepted manuscript made available via CHORUS. The article has been published as:

Stationary current between hybrid vibrational polaritonic systems

Kenneth A. Jung and Junjie Liu

Phys. Rev. B **108**, L081404 — Published 8 August 2023

DOI: 10.1103/PhysRevB.108.L081404

Stationary Current between Hybrid Vibrational Polaritonic Systems

Kenneth A. Jung[1, *] and Junjie Liu[2, †]

[1]*Department of Chemistry, Stanford University, Stanford, California, 94305, USA*

[2]*Department of Physics, International Center of Quantum and Molecular Structures, Shanghai University, Shanghai, 200444, China*

(Dated: July 31, 2023)

Strong light-matter interaction and resulting polaritons provide a promising knob to control energy and population transfer over long length scales. Yet, existing transfer studies have been exclusively limited to a single cavity scenario. Little is known whether multiple cavities can facilitate new control strategies. Here we reveal that the interplay of cavity-cavity coherence and strong vibrational light-matter coupling can induce a stationary population current between two identical, weakly-coupled hybrid vibrational polaritonic systems at thermal equilibrium. Exploiting Fermi's Golden rule, we qualitatively identify that the current is mediated by transitions between vibrational polariton states belonging to different hybrid systems. Our results provide new insights for realizing controllable long-distance population transfer utilizing coupled light-matter hybrid systems.

Introduction.– Light-matter interaction is a cornerstone concept in many research disciplines, ranging from cavity and circuit quantum electrodynamics [1–3], optomechanics [4], to quantum thermodynamics [5, 6] and quantum chemistry [7–9]. To devise applications relying on the coherent effects of light-matter interaction, the light-matter coupling strength is increased continuously, reaching the strong coupling regime [10, 11] and beyond [12, 13]. As strong light-matter interaction allows for a coherent exchange of excitations between light and matter, it finds vital applications in quantum information science [14, 15], including fast quantum gate operations [16, 17], coherent frequency conversion [18, 19] and quantum networking [20, 21] to name just a few examples.

Strong light-matter interaction can also generate hybrid light-matter states known as polaritons [22] which bring forward new techniques for the manipulation of matter. Recent advances in experimental and theoretical research have demonstrated the possibility of controlling energy and population transfer by harnessing electronic or excitonic polaritons [23–36] and their vibrational counterparts [37–40]. Of particular interest are observations of polariton-mediated long range transfer [26, 28, 32, 38], and that the control can be achieved even with a vacuum electromagnetic field containing no photons [24]. This kind of controllable long-range transfer can promote the development of the emerging interdisciplinary quantum technologies [20, 21]. Nevertheless, existing studies [23–40] exclusively focused on hybrid scenarios with a single cavity which can potentially limit the transfer distance. On the other hand, coupled cavities are frequently utilized in quantum information processing [41–47] and quantum simulation [48, 49]. Combining coupled cavities and polaritons may open up new opportunities for realizing long-distance transfer, which remains, however, largely unexplored.

Here we investigate population transfer between coupled yet spatially separated hybrid vibrational polaritonic systems. Our model builds upon recent experimental platforms involving vibrational light-matter coupling [50, 51]. Treating the hybrid system as a whole and noting the conservation of population, we find that the population current between two hybrid systems is solely related to the cavity-cavity coherence. We demonstrate an interplay between the cavity-cavity coherence and strong vibrational light-matter interaction in supporting a nonzero stationary population current between identical hybrid systems. We resort to Fermi's Golden rule in the regime of its validity to pinpoint the underlying origin of this nonzero population current. Through the agreements in trends, we argue that the population current is mediated by transitions between polariton states belonging to different hybrid systems.

Our results reveal new features of population transfer in vibrational polaritonic systems. As compared with existing studies [23–40], the opening of a transfer channel in our setup relies on both a finite cavity-cavity coupling and the formation of polariton states. Furthermore, our results provide a way to control long-range transfer utilizing cavity-cavity coherence in a multiple cavity scenario and particularly, indicate a possibility of extending the spatial distance of polariton-assisted transfer by noting that the spatial separation between two adjacent cavities is about 47μm in Ref. [50]. For comparison, a transfer distance of 7μm is achieved in another existing study [26] using a single cavity.

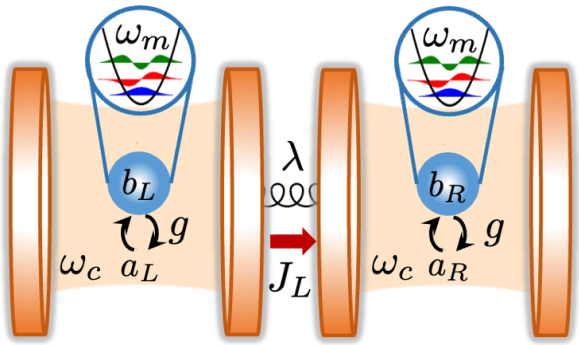


Figure 1. Depiction of the setup. It consists of two identical hybrid vibrational polaritonic systems held at the same temperature, each containing a cavity with frequency ω_c and a molecule with frequency ω_m. The left and right cavities interact via a photon-hopping coupling with a strength λ. When the vibrational light-matter coupling, measured by g, is turned on a stationary population current proportional to the coherence between the two cavities can emerge.

Coupled hybrid polariton systems.– We consider a light-matter hybrid system as schematically depicted in Fig. 1. The

total Hamiltonian consists of three parts (setting $\hbar = 1$ and $k_B = 1$ hereafter)

$$H = H_M + H_C + H_{M-C}. \tag{1}$$

The molecular Hamiltonian H_M accounts for the primary vibrations of two single molecules described by harmonic oscillators of frequencies $\omega_{L,R}$ (valid for small displacements, see, e.g., Ref. [52]) with annihilation operators $b_{L,R}$ and their individual vibrational environments in the left (L) and right (R) cavities

$$H_M = \sum_{i=L,R} \omega_i b_i^\dagger b_i + \sum_{i=L,R} \int_0^\infty d\Omega\, \Omega\, r_{\Omega,i}^\dagger r_{\Omega,i} + \sum_{i=L,R} \int_0^\infty d\Omega \sqrt{\frac{\gamma_i(\Omega)}{2\pi}} (r_{\Omega,i}^\dagger b_i + b_i^\dagger r_{\Omega,i}), \tag{2}$$

The vibrational environment for each molecule contains a continuum of harmonic oscillators with annihilation operators $r_{\Omega,i}^\dagger$. The parameter $\gamma_i(\Omega)$ denotes a frequency-dependent coupling coefficient between the molecule in the ith cavity and its vibrational environment. The detailed values of $\{\gamma_i(\Omega)\}$ are encoded in a super-Ohmic spectrum $\gamma_i(\Omega) = \gamma_i \Omega^3 \exp(-\Omega/\Omega_{\rm cut})/\Omega_{\rm cut}^2$ with γ_i a dimensionless coupling strength and $\Omega_{\rm cut}$ a cut-off frequency, assumed to be the same for the two molecules.

The cavity Hamiltonian H_C describes two spatially separated cavities, each supports a dispersionless cavity mode of frequency $\omega_{c,i}$ with annihilation operator a_i, and their coupling measured by a coupling strength λ, as well as a continuum of radiative far-field photon modes $f_{\varpi,i}^\dagger$ and their coupling to the cavity modes,

$$H_C = \sum_{i=L,R} \omega_{c,i} a_i^\dagger a_i + \lambda (a_L^\dagger a_R + a_R^\dagger a_L) + \sum_{i=L,R} \int_0^\infty d\varpi\, \varpi f_{\varpi,i}^\dagger f_{\varpi,i} + \sum_{i=L,R} \int_0^\infty d\varpi \sqrt{\frac{\kappa_i(\varpi)}{4\pi}} (f_{\varpi,i}^\dagger a_i + a_i^\dagger f_{\varpi,i}). \tag{3}$$

We determine frequency-dependent coupling coefficients $\{\kappa_i(\varpi)\}$ from a super-Ohmic spectrum [53] $\kappa_i(\varpi) = \kappa_i \varpi^3 \exp(-\varpi/\varpi_{\rm cut})/\varpi_{\rm cut}^2$ with κ_i a dimensionless coupling strength and $\varpi_{\rm cut}$ a cut-off frequency. The final term, H_{M-C} describes the potentially strong interaction between molecular vibrations and their respective cavity photon modes treated within the rotating wave approximation

$$H_{M-C} = \sum_{L,R} g_i (a_i^\dagger b_i + b_i^\dagger a_i), \tag{4}$$

where g_i is the vibrational light-matter coupling strength. We set the temperatures of the vibrational environments and far-field photon baths to be the same such that the entire system is in thermal equilibrium at temperature T. Extensions to cases where each bath is at a unique temperature is straightforward in what follows. Here we limit ourselves to identical hybrid systems with $\omega_{L,R} = \omega_m$, $\omega_{c,L/R} = \omega_c$, $\gamma_{L,R} = \gamma$, $\kappa_{L,R} = \kappa$ and $g_{L,R} = g$ and relegate an analysis for coupled non-identical hybrid systems to the supplemental materials (SM) [54].

Stationary population current.– We note that the population of the composite system is conserved thereby allowing for the proper definition of a population current. Starting from the conservation of excitation number in the total system

$$\sum_{i=L,R} \mathcal{P}_i = \text{Constant}, \tag{5}$$

where the number operator is defined as $\mathcal{P}_i = b_i^\dagger b_i + a_i^\dagger a_i + \int d\Omega r_{\Omega,i}^\dagger r_{\Omega,i} + \int d\varpi f_{\varpi,i}^\dagger f_{\varpi,i}$, we take a time derivative over both sides of Eq. (5) and define a stationary population current with respect to the ith hybrid system $J_i = \langle \dot{\mathcal{P}}_i \rangle$ with an average taken with respect to an initial factorized state for cavity modes, molecules and their thermal environments in the Heisenberg picture [54].

In our modeling, we explicitly take the photon bath and vibrational environment into account, we hence utilize the generalized input-output method [55, 56] to solve dynamics. Introducing the generalized input fields $b_i^{\rm in} = \int_0^\infty d\Omega \sqrt{\frac{\gamma_i(\Omega)}{2\pi}} e^{-i\Omega(t-t_0)} r_{\Omega,i}(t_0)$ and $a_i^{\rm in} = \int_0^\infty d\varpi \sqrt{\frac{\kappa_i(\varpi)}{4\pi}} e^{-i\varpi(t-t_0)} f_{\varpi,i}(t_0)$ with the initial time $t_0 \to -\infty$, we define EOMs for the relevant operators from which we find that the population current for the left hybrid system turns out to be

$$J_L = 2\lambda \text{Im}\langle a_L^\dagger a_R \rangle. \tag{6}$$

We relegate derivation details to the SM [54]. From Eq. (6) it is clear that the population current is directly related to the imaginary (Im) part of the cavity-cavity coherence with the magnitude further controlled by the cavity-cavity coupling strength λ. We remark that this formal current definition ensures a vanishing net current $\sum_{i=L,R} J_i = 0$ with J_R obtained by exchanging the indices.

To enable a straightforward numerical evaluation of the population current defined in Eq. (6) we need the explicit time evolution of a_L and a_R. Introducing vectors $u = (b_L, a_L, a_R, b_R)^T$ and $u^{\rm in} = (b_L^{\rm in}, a_L^{\rm in}, a_R^{\rm in}, b_R^{\rm in})^T$, we can cast the EOMs in a matrix form [54]

$$\frac{d}{dt} u(t) = -iMu(t) - iu^{\rm in}(t), \tag{7}$$

where the drift matrix reads

$$M = \begin{pmatrix} \tilde{\omega}_m & g & 0 & 0 \\ g & \tilde{\omega}_c & \lambda & 0 \\ 0 & \lambda & \tilde{\omega}_c & g \\ 0 & 0 & g & \tilde{\omega}_m \end{pmatrix}. \tag{8}$$

Here, we have introduced the complex frequencies $\tilde{\omega}_m = \omega_m - i\Gamma/2$ and $\tilde{\omega}_c = \omega_c - iK/4$ with $\Gamma \equiv \gamma(\omega_m)$ and $K \equiv \kappa(\omega_c)$ being effective damping strengths experienced by the primary modes b_L and a_L, respectively. We now formally introduce

the matrix R whose rows are comprised of the left eigenvectors of the drift matrix M satisfying $R \cdot M = \Lambda \cdot R$ with Λ a diagonal matrix that contains the eigenvalues of M. By doing so, we can obtain a formal solution of Eq. (7)

$$u(t) = -i \int_{-\infty}^{t} d\tau \mathcal{A}(t-\tau) u^{\text{in}}(\tau), \tag{9}$$

with the matrix $\mathcal{A}(t) \equiv R^{-1} \cdot e^{-i\Lambda t} \cdot R$. It is then straightforward to show

$$J_L = 2\lambda \sum_{k=1}^{4} \text{Im}\Big\{ \int_{-\infty}^{t} d\tau \int_{-\infty}^{t} d\tau' \mathcal{A}_{2k}^{*}(t-\tau)\mathcal{A}_{3k}(t-\tau') \times \langle u_k^{\text{in},\dagger}(\tau) u_k^{\text{in}}(\tau') \rangle \Big\}. \tag{10}$$

Here, $\mathcal{A}_{nm}(t)$ represents an element of the matrix $\mathcal{A}(t)$ with $\mathcal{A}_{nm}^{*}(t)$ its complex conjugate. Finite temperature effects enter into the current expression through correlations of the input fields $\langle u_k^{\text{in},\dagger}(\tau) u_k^{\text{in}}(\tau') \rangle$ which can be exactly evaluated using initial Bose-Einstein distributions for bosonic baths [55]. An expanded version of Eq. (10) that is used for numerical evaluation is shown in the SM [54].

One may expect that $\lambda \neq 0$ is sufficient for supporting a nonzero population current. However, for coupled identical hybrid systems, we can use Eq. (10) to analytically prove that $g \neq 0$ is also required for having $J_L \neq 0$; For $g = 0$ and $\lambda \neq 0$, the cavity-cavity coherence $\langle a_L^{\dagger} a_R \rangle$ is real valued and the population current vanishes altogether [54]. Only when $g, \lambda \neq 0$, does the cavity-cavity coherence possesses an imaginary part. Hence, for coupled identical hybrid systems, a nonzero population current requires an interplay of the cavity-cavity coherence and vibrational light-matter coupling, which is one of the main results of the present study.

Fig. 2 shows population current results marked by red solid lines obtained from Eq. (10). From Fig. 2 (a), we find that J_L is a nonlinear and monotonic increasing function of the cavity-cavity coupling strength λ under a fixed light-matter coupling strength g. From Eq. (8), we know the matrix elements $\mathcal{A}_{mn}$ depend on λ. Treating the weak cavity-cavity coupling as a perturbation within the drift matrix $M = M_0 + \lambda M_1$; Non-vanishing matrix elements of M_1 are $[M_1]_{32} = [M_1]_{23} = 1$, we can approximate $\Lambda = \Lambda_0 + \lambda\Lambda_1 + \mathcal{O}(\lambda^2)$ with $\Lambda_{0(1)}$ the zeroth (first)-order contribution to eigenvalues of the drift matrix M, and corresponding eigenvectors $R = R_0 + \lambda R_1 + \mathcal{O}(\lambda^2)$ with $R_{0(1)}$ containing zeroth (first)-order eigenvector contributions as rows. Similarly, $R^{-1} = R_0^{-1}/(1 + \lambda R_1/R_0 + \cdots) \approx R_0^{-1}(1 - \lambda R_1/R_0) + \cdots$. We get that $\mathcal{A} = R_0^{-1} e^{-i\Lambda_0 t} R_0 + \lambda(R_0^{-1} e^{-i\Lambda_0 t} R_1 - R_1 R_0^{-2} e^{-i\Lambda_0 t} R_0) + \cdots$ from which one finds the cavity-cavity coherence vanishes when $\lambda = 0$. We then infer that $\langle a_L^{\dagger} a_R \rangle \propto \lambda$ to the lowest-order of λ, therefore, the population current $J_L \propto \lambda^2$ depends *quadratically* on λ to the lowest-order.

We now turn our attention to assessing the behavior of the current as the light-matter coupling strength is tuned in Fig. 2 (b). For the chosen parameters the effective damping strengths $K, \Gamma \sim 2 \times 10^{-4}$ thereby determining the strong coupling

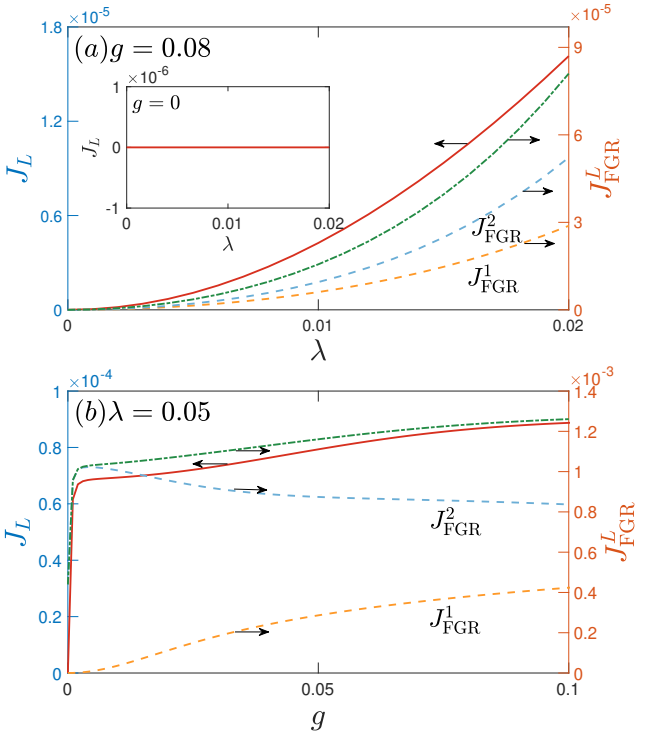


Figure 2. Results for the population current J_L (left axis, red solid lines) defined in Eq. (10) and FGR current J_{FGR}^L (right axis, green dashed-dotted lines) as given by Eq. (11). (a) Currents as a function of the cavity-cavity coupling λ with a fixed light-matter interaction strength $g = 0.08$. The inset shows $J_L = 0$ when $g = 0$ regardless of the cavity-cavity coupling. (b) Currents as a function of the light-matter interaction strength g with a fixed cavity-cavity coupling $\lambda = 0.05$. The dashed lines in both plots mark results for components J_{FGR}^1 (orange) and J_{FGR}^2 (blue). Other dimensionless parameters are $\omega_m = 0.95$, $\omega_c = 0.9$, $T = 0.5$, $\gamma = 0.03$, $\kappa = 0.03$ and $\Omega_{\text{cut}} = \varpi_{\text{cut}} = 10$.

regime of $g > K, \Gamma$. The first notable feature is a sharp initial rise in the current when entering into the strong coupling regime regardless of the cavity-cavity coupling strength. After the initial rise increasing the light-matter coupling strength g only mildly increases the current. In the SM [54] we compare current results between coupled hybrid systems with identical and non-identical cavities when varying g. Due to resonance, we generally find that identical cavities give rise to larger currents than non-identical cavities regardless of the values of g and λ by at least an order of magnitude. This situation is similar to what is found in three-level V-type systems[57, 58].

Fermi's golden rule picture.– While Eq. (10) yields a compact expression for numerical treatment it is unwieldy for pinpointing the underlying origins of the observed behavior of the current. Noting the quadratic dependence of J_L on λ, we resort to Fermi's golden rule (FGR) to gain physical insight in the limit of weak cavity-cavity coupling as compared to the effective Rabi splitting $\Omega_R = \sqrt{(\omega_m - \omega_c)^2 + 4g^2}$. Upon neglecting the vibrational and photonic environments, we decompose the remaining Hamiltonian $H' = H_0 + V$ with V con-

taining only the cavity-cavity coupling term. We develop the FGR picture explicitly in the basis of polariton states which diagonalizes H_0 in the strong coupling regime. By doing so, we expect that the FGR picture will be suitable for capturing trends but should be used with caution when analyzing the magnitude of J_L and its behavior in the weak light-matter coupling regime. A finite V induces transitions between left and right polariton states with annihilation operators $U_{L,R}$ and $L_{L,R}$ corresponding to upper and lower branches, respectively.

Using the Born expansion, we define the lowest-order FGR transition rate between polariton states as $P_{i\to f} = |\langle f|V|i\rangle|^2$. Explicitly, we have $P_{U\to\tilde{U}} = \lambda^2 \sin^4\theta$, $P_{L\to\tilde{L}} = \lambda^2\cos^4\theta$ and $P_{U\to\tilde{L}} = P_{L\to\tilde{U}} = \frac{\lambda^2}{4}\sin^2(2\theta)$. Here, $\tilde{U}$ and $\tilde{L}$ mark polariton states on the opposite side with respect to U and L and the angle θ satisfies the relation $\tan(2\theta) = 2g/(\omega_m - \omega_c)$; see the SM [54] for details. We introduce the FGR population current as

$$J^L_{\rm FGR} = \sum_{i\in\{U,L\},f\in\{\tilde{U},\tilde{L}\}} P_{i\to f}\cdot\langle i^\dagger_L i_L\rangle. \tag{11}$$

Here, $\langle U^\dagger_L U_L\rangle$ and $\langle L^\dagger_L L_L\rangle$ are the steady-state populations of the left upper and lower polariton states, respectively. We can obtain these populations using the solutions given in Eq. (9) [54]. To distinguish the transport channels, we further decompose $J^L_{\rm FGR} = J^1_{\rm FGR} + J^2_{\rm FGR}$ with $J^1_{\rm FGR} = \sum_{i=U,f\in\{\tilde{U},\tilde{L}\}} P_{i\to f}\cdot\langle i^\dagger_L i_L\rangle$ and $J^2_{\rm FGR} = \sum_{i=L,f\in\{\tilde{U},\tilde{L}\}} P_{i\to f}\cdot\langle i^\dagger_L i_L\rangle$ marking flux contributions from the transitions out of the upper and the lower polaritons respectively to the polariton states on the opposite side.

To check the validity of the FGR picture, we benchmark $J^L_{\rm FGR}$ against J_L in Fig. 2. From Fig. 2 (a), we observe that $J^L_{\rm FGR}$ does a reasonable job at capturing the nonlinear trend of the current computed from Eq. (10) by noting that transition rates depend quadratically on λ. The contributions $J^1_{\rm FGR}$ and $J^2_{\rm FGR}$ to the total current are roughly equal at small values of λ. As the cavity-cavity coupling strength is increased the $J^1_{\rm FGR}$ contribution becomes more pronounced indicating that the channel responsible for transferring population from the upper polariton branch is beginning to dominate the current.

Turning to the scenario of varying the light-matter coupling strength g, we still observe that $J^L_{\rm FGR}$ is capable of capturing the basic trend of J_L as can be seen from Fig. 2 (b). From the comparison, we can infer that the initial fast rise in J_L can be attributed to the transitions starting from the lower polariton branch. As g increases, $J^2_{\rm FGR}$ will reach a maximum and then decreases, while the $J^1_{\rm FGR}$ contribution is monotonically increasing, resulting in the slow increasing trend of J_L. Albeit the success of $J^L_{\rm FGR}$ in capturing the subtle trends of J_L, we note that the simple FGR current fails in correctly predicting the vanishing current when $g = 0$ (see also inset of Fig. 2 (a)) as well as the magnitude of J_L. This is expected since we (i) neglected the environmental parts which play a role in defining J_L and (ii) defined $J^L_{\rm FGR}$ in the basis of polariton states which becomes inapplicable when $g = 0$. Thus the so-developed FGR picture should be understood in a qualitative manner.

Discussion.– Here we considered a single molecule in each cavity for analytical clarity, similar in spirit to previous theoretical studies [59, 60]. We remark that our findings should hold in the collective coupling regime involving an ensemble of N molecules in each cavity. Noting the linear nature of EOMs listed in the SM [54] and defining the current with respect to a modified number operator $\mathcal{P}_L = \sum_{k=1}^N \left(b^\dagger_{kL}b_{kL} + \int d\Omega r^\dagger_{\Omega,kL}r_{\Omega,kL}\right) + a^\dagger_L a_L + \int d\varpi f^\dagger_{\varpi,L}f_{\varpi,L}$, one can find that the population current still adopts the form of Eq. (6). Eqs. (7)-(9) can also be easily generalized to include N molecules. Though the light-matter coupling strength can be enhanced by a factor of $\sqrt{N}$ in the collective coupling regime, the presence of dark states may suppress transfer processes [52]. We have neglected the anharmonic nature of the molecular vibrational modes and those that may arise in the couplings. While we expect these to have little effect on the validity of our findings they may give further control over the population transfer in these types of systems which we leave for future investigation.

Our setup is experimentally feasible. We note that a single-molecule nanocavity is already within the current experimental capabilities [51]. Extending to the collective coupling regime, one may directly adopt an experimental platform [50] in which the authors successfully fabricated an array of Fabry-Perot cavities coupled through photon-hopping processes. Strong vibrational light-matter coupling is achieved with $\omega_m = 1983\ \mathrm{cm}^{-1}$ and $\omega_c = 1970, 2000\ \mathrm{cm}^{-1}$, and interactions between polarition states contained in different hybrid systems is demonstrated using two-dimensional infrared spectroscopy [50]. Moreover, frequencies of the cavities can be experimentally tuned by modulating their thickness [50], allowing for verification of our findings from coupled hybrid systems with identical to non-identical cavities. By noting that the separation between two adjacent cavities is about 47μm [50], we suggest that by using multiple coupled cavities one can significantly extend the spatial range of polariton-mediated transfer, providing advantages over single-cavity scenarios.

In summary, we have addressed population transfer between hybrid vibrational polaritonic systems. We found that transitions between polariton states contained in different hybrid systems can mediate a nonzero stationary population current which has a quadratic leading order scaling in the cavity-cavity coupling strength. Our setup can serve as a building block for studying long-range transfer in a lattice of coupled hybrid systems in the near future.

Acknowledgement.– K.A.J acknowledges support from the National Science Foundation Grant No. CHE-2154291. J. Liu acknowledges supports from the National Natural Science Foundation of China (Grant No. 12205179), Shanghai Pujiang Program (Grant No. 22PJ1403900) and start-up funding of Shanghai University.

* kajung@stanford.edu
† jjliu.fd@gmail.com

[1] A. A. Clerk, K. W. Lehnert, P. Bertet, J. R. Petta, and Y. Nakamura, "Hybrid quantum systems with circuit quantum electrodynamics," Nat. Phys. , 257 (2020).
[2] G. Burkard, M. J. Gullans, X. Mi, and J. R. Petta, "Superconductor-semiconductor hybrid-circuit quantum electrodynamics," Nat. Rev. Phys. , 129 (2020).
[3] A. Blais, A. L. Grimsmo, S. M. Girvin, and A. Wallraff, "Circuit quantum electrodynamics," Rev. Mod. Phys. **93**, 025005 (2021).
[4] M. Aspelmeyer, T. J. Kippenberg, and F. Marquardt, "Cavity optomechanics," Rev. Mod. Phys. **86**, 1391 (2014).
[5] J.P. Pekola and I.M. Khaymovich, "Thermodynamics in single-electron circuits and superconducting qubits," Annu. Rev. Condens. Matter Phys. **10**, 193 (2019).
[6] Jiteng S., Cheng Y., and Haibin W., "Realization of a coupled-mode heat engine with cavity-mediated nanoresonators," Sci. Adv. **7**, eabl7740 (2021).
[7] J. Flick, M. Ruggenthaler, H. Appel, and A. Rubio, "Atoms and molecules in cavities, from weak to strong coupling in quantum-electrodynamics (QED) chemistry," Proc. Natl. Acad. Sci. U.S.A. **114**, 3026 (2017).
[8] R. F. Ribeiro, L. Martínez-Martínez, M. Du, J. Campos-Gonzalez-Angulo, and J. Yuen-Zhou, "Polariton chemistry: controlling molecular dynamics with optical cavities," Chem. Sci. **9**, 6325 (2018).
[9] K. Nagarajan, A. Thomas, and T. W. Ebbesen, "Chemistry under vibrational strong coupling," J. Am. Chem. Soc. **143**, 16877 (2021).
[10] Y. Kaluzny, P. Goy, M. Gross, J. M. Raimond, and S. Haroche, "Observation of self-induced rabi oscillations in two-level atoms excited inside a resonant cavity: The ringing regime of superradiance," Phys. Rev. Lett. **51**, 1175 (1983).
[11] R. J. Thompson, G. Rempe, and H. J. Kimble, "Observation of normal-mode splitting for an atom in an optical cavity," Phys. Rev. Lett. **68**, 1132 (1992).
[12] P. Forn-Díaz, L. Lamata, E. Rico, J. Kono, and E. Solano, "Ultrastrong coupling regimes of light-matter interaction," Rev. Mod. Phys. **91**, 025005 (2019).
[13] A. Frisk Kockum, A. Miranowicz, S. De Liberato, S. Savasta, and F. Nori, "Ultrastrong coupling between light and matter," Nat. Rev. Phys. **1**, 19 (2019).
[14] A. Blais, S. M. Girvin, and W. D. Oliver, "Quantum information processing and quantum optics with circuit quantum electrodynamics," Nat. Phys. , 247 (2020).
[15] S. Barzanjeh, A. Xuereb, S. Gröblacher, M. Paternostro, C. A. Regal, and E. M. Weig, "Optomechanics for quantum technologies," Nat. Phys. **18**, 15 (2022).
[16] G. Romero, D. Ballester, Y. M. Wang, V. Scarani, and E. Solano, "Ultrafast quantum gates in circuit qed," Phys. Rev. Lett. **108**, 120501 (2012).
[17] Y. Wang, C. Guo, G.-Q. Zhang, G. Wang, and C. Wu, "Ultrafast quantum computation in ultrastrongly coupled circuit qed systems," Sci. Rep. **7**, 44251 (2017).
[18] M. Mirhosseini, A. Sipahigil, M. Kalaee, and O. Painter, "Superconducting qubit to optical photon transduction," Nature **588**, 599 (2020).
[19] M. Forsch, R. Stockill, A. Wallucks, I. Marinković, C. Gärtner, R. A. Norte, F. van Otten, A. Fiore, K. Srinivasan, and S. Gröblacher, "Microwave-to-optics conversion using a mechanical oscillator in its quantum ground state," Nat. Phys. **16**, 69 (2020).
[20] C. Simon, "Towards a global quantum network," Nat. Photonics **11**, 678 (2017).
[21] S. Wehner, D. Elkouss, and R. Hanson, "Quantum internet: A vision for the road ahead," Science **362** (2018), 10.1126/science.aam9288.
[22] T. W. Ebbesen, "Hybrid light–matter states in a molecular and material science perspective," Acc. Chem. Res. **49**, 2403 (2016).
[23] D. Coles, N. Somaschi, P. Michetti, C. Clark, P. Lagoudakis, P. Savvidis, and D. Lidzey, "Polariton-mediated energy transfer between organic dyes in a strongly coupled optical microcavity," Nat. Mater. **13**, 712 (2014).
[24] E. Orgiu, J. George, J. A. Hutchison, E. Devaux, J. F. Dayen, B. Doudin, F. Stellacci, C. Genet, J. Schachenmayer, C. Genes, G. Pupillo, P. Samori, and T. W. Ebbesen, "Conductivity in organic semiconductors hybridized with the vacuum field," Nat. Mater. **14**, 1123 (2015).
[25] J. Schachenmayer, C. Genes, E. Tignone, and G. Pupillo, "Cavity-enhanced transport of excitons," Phys. Rev. Lett. **114**, 196403 (2015).
[26] D. Bouchet, D. Cao, R. Carminati, Y. De Wilde, and V. Krachmalnicoff, "Long-range plasmon-assisted energy transfer between fluorescent emitters," Phys. Rev. Lett. **116**, 037401 (2016).
[27] X. Zhong, T. Chervy, S. Wang, J. George, A. Thomas, J. A. Hutchison, E. Devaux, C. Genet, and T. W. Ebbesen, "Non-radiative energy transfer mediated by hybrid light-matter states," Angew. Chem. Int. Ed. **55**, 6202 (2016).
[28] X. Zhong, T. Chervy, L. Zhang, A. Thomas, J. George, C. Genet, J. A. Hutchison, and T. W. Ebbesen, "Energy transfer between spatially separated entangled molecules," Angew. Chem. Int. Ed. **56**, 9034 (2017).
[29] F. Herrera and F. C. Spano, "Cavity-controlled chemistry in molecular ensembles," Phys. Rev. Lett. **116**, 238301 (2016).
[30] D. Hagenmüller, J. Schachenmayer, S. Schütz, C. Genes, and G. Pupillo, "Cavity-enhanced transport of charge," Phys. Rev. Lett. **119**, 223601 (2017).
[31] D. Hagenmüller, S. Schütz, J. Schachenmayer, C. Genes, and G. Pupillo, "Cavity-assisted mesoscopic transport of fermions: Coherent and dissipative dynamics," Phys. Rev. B **97**, 205303 (2018).
[32] R. Sáez-Blázquez, J. Feist, A. I. Fernández-Domínguez, and F. J. García-Vidal, "Organic polaritons enable local vibrations to drive long-range energy transfer," Phys. Rev. B **97**, 241407 (2018).
[33] D. M. Myers, S. Mukherjee, J. Beaumariage, D. W. Snoke, M. Steger, L. N. Pfeiffer, and K. West, "Polariton-enhanced exciton transport," Phys. Rev. B **98**, 235302 (2018).
[34] M. Reitz, F. Mineo, and C. Genes, "Energy transfer and correlations in cavity-embedded donor-acceptor configurations," Sci. Rep. **8**, 9050 (2018).
[35] C. Schäfer, M. Ruggenthaler, H. Appel, and A. Rubio, "Modification of excitation and charge transfer in cavity quantum-electrodynamical chemistry," Proc. Natl. Acad. Sci. U.S.A. **116**, 4883 (2019).
[36] G. Arwas and C. Ciuti, "Quantum electron transport controlled by cavity vacuum fields," Phys. Rev. B **107**, 045425 (2023).
[37] J. A. Campos-Gonzalez-Angulo, R. F. Ribeiro, and J. Yuen-Zhou, "Resonant catalysis of thermally activated chemical reactions with vibrational polaritons," Nat. Commun. **10**, 4685 (2019).
[38] M. Du, L. A. Martinez-Martinez, R. F. Ribeiro, Z. Hu, V. M.

Menon, and J. Yuen-Zhou, "Theory for polariton-assisted remote energy transfer," Chem. Sci. **9**, 6659 (2018).
[39] B. Xiang, R. F. Ribeiro, M. Du, L. Chen, Z. Yang, J. Wang, J. Yuen-Zhou, and W. Xiong, "Intermolecular vibrational energy transfer enabled by microcavity strong light–matter coupling," Science **368**, 665 (2020).
[40] T. E. Li, A. Nitzan, and J. E. Subotnik, "Collective vibrational strong coupling effects on molecular vibrational relaxation and energy transfer: Numerical insights via cavity molecular dynamics simulations," Angew. Chem. Int. Ed. **60**, 15533 (2021).
[41] S. Giampaolo and F. Illuminati, "Long-distance entanglement and quantum teleportation in coupled-cavity arrays," Phys. Rev. A **80**, 050301 (2009).
[42] F. Nissen, S. Schmidt, M. Biondi, G. Blatter, H. E. Türeci, and J. Keeling, "Nonequilibrium dynamics of coupled qubit-cavity arrays," Phys. Rev. Lett. **108**, 233603 (2012).
[43] J. Jin, D. Rossini, R. Fazio, M. Leib, and M. J. Hartmann, "Photon solid phases in driven arrays of nonlinearly coupled cavities," Phys. Rev. Lett. **110**, 163605 (2013).
[44] T. Liew and V. Savona, "Multimode entanglement in coupled cavity arrays," New J. Phys. **15**, 025015 (2013).
[45] S. Felicetti, G. Romero, D. Rossini, R. Fazio, and E. Solano, "Photon transfer in ultrastrongly coupled three-cavity arrays," Phys. Rev. A **89**, 013853 (2014).
[46] G. Almeida, F. Ciccarello, T. Apollaro, and A. Souza, "Quantum-state transfer in staggered coupled-cavity arrays," Phys. Rev. A **93**, 032310 (2016).
[47] W. Qin and F. Nori, "Controllable single-photon transport between remote coupled-cavity arrays," Phys. Rev. A **93**, 032337 (2016).
[48] Helmut Ritsch, Peter Domokos, Ferdinand Brennecke, and Tilman Esslinger, "Cold atoms in cavity-generated dynamical optical potentials," Rev. Mod. Phys. **85**, 553 (2013).
[49] M. J Hartmann, "Quantum simulation with interacting photons," J. Opt. **18**, 104005 (2016).
[50] B. Xiang, J. Wang, Z. Yang, and W. Xiong, "Nonlinear infrared polaritonic interaction between cavities mediated by molecular vibrations at ultrafast time scale," Sci. Adv. **7**, eabf6397 (2021).
[51] E. A. Muller, B. Pollard, H. A. Bechtel, R. Adato, D. Etezadi, H. Altug, and M. B. Raschke, "Nanoimaging and control of molecular vibrations through electromagnetically induced scattering reaching the strong coupling regime," ACS Photonics **5**, 3594 (2018).
[52] Matthew Du and Joel Yuen-Zhou, "Catalysis by dark states in vibropolaritonic chemistry," Phys. Rev. Lett. **128**, 096001 (2022).
[53] J. del Pino, F. Schröder, A. W. Chin, J. Feist, and F. J. Garcia-Vidal, "Tensor network simulation of non-markovian dynamics in organic polaritons," Phys. Rev. Lett. **121**, 227401 (2018).
[54] See Supplemental Material for derivation details for the population current, the proof of a vanishing current between identical hybrid systems when the light-matter interaction is turned off, details of implementing Fermi's Golden rule and complementary numerical results for non-identical hybrid systems.
[55] J. Liu and D. Segal, "Generalized input-output method to quantum transport junctions. I. general formulation," Phys. Rev. B **101** (2020), 10.1103/physrevb.101.155406.
[56] J. Liu and D. Segal, "Generalized input-output method to quantum transport junctions. II. applications," Phy. Rev. B **101** (2020), 10.1103/physrevb.101.155407.
[57] T. V. Tscherbul and P. Brumer, "Non-equilibrium stationary coherences in photosynthetic energy transfer under weak-field incoherent illumination," J. Chem. Phys. **148**, 124114 (2018).
[58] K. A. Jung and P. Brumer, "Energy transfer under natural incoherent light: Effects of asymmetry on efficiency," J. Chem. Phys. **153**, 114102 (2020).
[59] M. A. D. Taylor, A. Mandal, W. Zhou, and P. Huo, "Resolution of gauge ambiguities in molecular cavity quantum electrodynamics," Phys. Rev. Lett. **125**, 123602 (2020).
[60] C. Schäfer, J. Flick, E. Ronca, P. Narang, and A. Rubio, "Shining light on the microscopic resonant mechanism responsible for cavity-mediated chemical reactivity," Nat. Commun. **13**, 7817 (2022).